In Vivo Tumor Cell Targeting with "Click" Nanoparticles

Geoffrey von Maltzahn,[†,‡] Yin Ren,[†,‡] Ji-Ho Park,[||] Dal-Hee Min,[‡] Venkata Ramana Kotamraju,[§] Jayanthi Jayakumar,[‡] Valentina Fogal,[§] Michael J. Sailor,[||] Erkki Ruoslahti,[§] and Sangeeta N. Bhatia*[,‡,⊥]

Harvard-MIT Division of Health Sciences and Technology, Cambridge, Massachusetts, Cancer Research Center, Burnham Institute for Medical Research, La Jolla, California, Vascular Mapping Center, Burnham Institute for Medical Research at University of California Santa Barbara, Santa Barbara, California, Materials Science and Engineering Program, Department of Chemistry and Biochemistry, University of California, San Diego, La Jolla, California 92093, and Electrical Engineering and Computer Science, MIT/Brigham & Women's Hospital, Boston, Massachusetts. Received March 3, 2008; Revised Manuscript Received May 7, 2008

The *in vivo* fate of nanomaterials strongly determines their biomedical efficacy. Accordingly, much effort has been invested into the development of library screening methods to select targeting ligands for a diversity of sites *in vivo*. Still, broad application of chemical and biological screens to the *in vivo* targeting of nanomaterials requires ligand attachment chemistries that are generalizable, efficient, covalent, orthogonal to diverse biochemical libraries, applicable under aqueous conditions, and stable in *in vivo* environments. To date, the copper(I)-catalyzed Huisgen 1,3-dipolar cycloaddition or "click" reaction has shown considerable promise as a method for developing targeted nanomaterials *in vitro*. Here, we investigate the utility of "click" chemistry for the *in vivo* targeting of inorganic nanoparticles to tumors. We find that "click" chemistry allows cyclic LyP-1 targeting peptides to be specifically linked to azido-nanoparticles and to direct their binding to p32-expressing tumor cells *in vitro*. Moreover, "click" nanoparticles are able to stably circulate for hours *in vivo* following intravenous administration (>5 h circulation time), extravasate into tumors, and penetrate the tumor interstitium to specifically bind p32-expressing cells in tumors. In the future, *in vivo* use of "click" nanomaterials should expedite the progression from ligand discovery to *in vivo* evaluation and diversify approaches toward multifunctional nanoparticle development.

INTRODUCTION

The ability to target nanomaterials to precise biological locations would have wide-ranging impact in biology and medicine. In living systems, highly controlled transportation networks continually shuttle payloads to and from specific molecular addresses. The efficiency of these systems provides strong motivation for the advancement of targeted nanoparticle technologies, particularly for the diagnosis and treatment of human diseases. Toward this goal, high throughput strategies for ligand discovery have generated a multitude of chemical and biological motifs with the potential to direct nanomaterials to specific biomolecular targets. However, translation of these ligands toward *in vivo* nanoparticle targeting has been limited by the number of nanoparticle attachment methods that are efficient, generalizable, aqueous compatible, chemically orthogonal to broad ranges of functional groups, and suitable for *in vivo* applications.

Previous work has demonstrated that *in vivo* bacteriophage display may be used to select for peptide sequences that mimic the ability of endogenous shuttles to target vascular and parenchymal tissue addresses (*1–5*). Already, linear peptide candidates of phage screens, as well as small molecule targeting candidates, have been translated toward nanomaterial targeting (*6–9*), primarily via use of exogenous or nonessential thiols, carboxylic acids, or amines. Still, some of the most powerful targeting motifs developed to date are those that contain essential thiol, amine, and carboxyl groups, thereby prohibiting their specific attachment via traditional methods. In particular, conformationally constrained, disulfide-cyclized targeting peptides are desirable for their enhanced affinity to biological receptors (*10, 11*), and resistance to proteolytic degradation *in vivo* relative to their linear counterparts (*12, 13*). However, specific intramolecular cyclization makes it difficult to add exogenous cysteine residues, while essential amines and carboxyl groups prohibit selective conjugation via exogenous lysine, aspartic acid, or glutamic acid residues. Additionally, noncovalent methods of ligand attachment relying on hydrophobic or electrostatic effects, although widely used *in vitro* (*14–16*), are unlikely to remain stable in blood or to resist rapid clearance *in vivo*. Recently, copper(I)-catalyzed "click" chemistry has emerged as an extraordinarily selective chemistry and an attractive solution in applications where commonly used thiol-reactive (maleimide, 2-pyridyldithio, iodoacetyl) or amine-reactive (NHS, epoxy, aldehyde, EDC) chemistries are not suitable (*17*). *In vitro* "click" chemistry has been utilized to generate functionalized polymers, (*18–20*), surfaces (*21–23*), and nanoparticles (*24–32*), and meets the previously mentioned criteria for broad utility in nanoparticle functionalization (chemical orthogonality, aqueous efficiency, applicability for diverse substrates). However, the use of "click" nanoparticles for *in vivo* applications has not been investigated. Particularly, as opposed to small molecule reagents with circulation times on the order of minutes (*8*), ligand attachments on long circulating nanomaterials must remain stable against *in vivo* degradation for hours while nanoparticles circulate systemically and identify molecular targets.

* Correspondence should be addressed to Sangeeta N. Bhatia, MD, PhD; Director, Laboratory for Multiscale Regenerative Technologies; Massachusetts Institute of Technology; E19-502D Cambridge, MA 02139. Phone: 617-324-0221. E-mail: sbhatia@mit.edu.

[†] These authors contributed equally.

[‡] Harvard-MIT Division of Health Sciences and Technology.

[§] Cancer Research Center, Burnham Institute for Medical Research, and Vascular Mapping Center, Burnham Institute for Medical Research at University of California Santa Barbara.

[||] University of California, San Diego.

[⊥] MIT/Brigham & Women's Hospital.

10.1021/bc800077y CCC: $40.75
Published on Web 07/09/2008

Scheme 1. Design of a "Click" Nanoparticle That Targets Tumor Cells *in Vitro* and *in Vivo*[a]

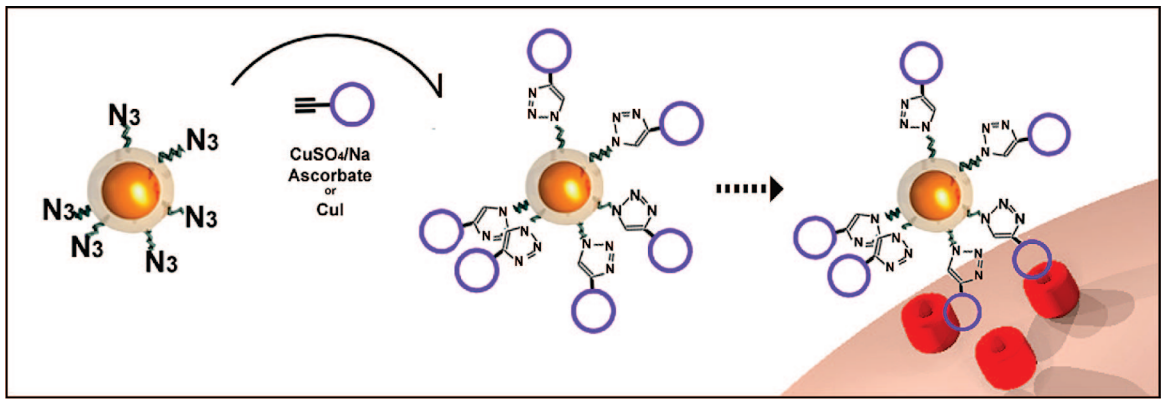

[a] Cross-linked, fluorescent, superparamagnetic iron oxide nanoparticles are modified to display azido-PEG groups. Conjugation of cyclic targeting peptides (purple circles) bearing pendant alkynes to azido-PEG nanoparticles via the copper(I)-catalyzed Huisgen 1,3-dipolar cycloaddition ("click" reaction) allows specific targeting of the nanoparticles to cells expressing the receptor (red).

Here, we find that alkyne-azide "click" chemistry provides a facile, single-step method for specifically linking the cyclic tumor-targeting peptide LyP-1 (CGNKRTRGC (*1, 33*);), which contains essential thiol and amine groups, to polymer-coated magnetofluorescent nanoparticles. LyP-1 binds to p32, a mitochondrial proteins that is both overexpressed and aberrantly localized at the cell surface of tumor cells, macrophages and lymphatic endothelial cells in certain experimental tumors and in human cancers (*34, 35*). We find that "click" LyP-1 nanoparticles are able stably traverse the systemic circulation, extravasate into tumors, and penetrate the tumor interstitium to specifically bind to receptors on p32-expressing cells in the tumors. Together, these results provide strong motivation for future use of "click" functionalization as a strategy for developing nanoparticles for *in vivo* biomedical applications (Scheme 1).

EXPERIMENTAL SECTION

Unless otherwise stated all reagents were purchased from Sigma-Aldrich and all reactions were performed at room temperature.

Iron Oxide Nanoparticle Synthesis. Cross-linked, aminated, fluorescent, superparamagnetic iron oxide nanoparticles were synthesized according to the published protocol (*36, 37*). Briefly, dextran-coated iron oxide nanoparticles were synthesized, purified, and subsequently cross-linked using epichlorohydrin. After exhaustive dialysis, particles were aminated by adding 1:10 v/v ammonium hydroxide (30%) and incubated on a shaker overnight. Aminated nanoparticles were subsequently purified from excess ammonia using a Sephadex G-50 column and concentrated using a high-gradient magnetic-field filtration column (Miltenyi Biotec). The near-infrared-fluorochrome VivoTag 680 was added to remotely detect particle accumulation *in vitro* and *in vivo* by reacting in 0.1 M HEPES buffer with 0.15 M NaCl at pH 7.2. DMSO-solubilized fluorochromes were added into particle solutions at 4 °C under mixing and allowed to warm to room temperature to react for 2 h. The yield was approximately 10 fluorochromes per nanoparticle for all experiments.

Succinimidyl 4-Azidobutyrate Synthesis (Scheme 2A). *Ethyl 4-azidobutyrate (***1***).* To a solution of ethyl 4-bromobutyrate (5.85 g, 30 mmol) in dimethyl sulfoxide (DMSO, 20 mL), sodium azide (2.925 g, 45 mmol) was added with stirring. The reaction mixture was stirred for 22 h at 55 °C, and cooled to room temperature. Water was added to the reaction mixture and extracted with ethyl ether (3 × 30 mL). The combined organic layer was washed with water and brine, and reduced in vacuo to afford 3.80 g of the azido compound **1**.

*4-Azidobutyric acid (***2***).* Ethyl 4-azidobutyrate **1** (3.14 g, 20 mmol) was dissolved in aqueous sodium hydroxide solution (1 N, 24 mL) with a minimum amount of methanol to make the solution homogeneous. The reaction mixture was stirred for 3 h at room temperature. After removal of methanol *in vacuo*, the aqueous solution was acidified to pH 0 with HCl and extracted with ethyl ether (3 × 50 mL). The ether layer was then dried over sodium sulfate and filtered. Removal of solvent gave the acid **2** (2.25 g).

*Succinimidyl 4-Azidobutyrate (***3***).* To a solution of *N*-hydroxyl succinimide (1.65 g, 14.3 mmol) in methylene chloride (100 mL) was added acid **2** (1.68 g, 13 mmol) followed by 1-ethyl-3-[3-dimethylaminopropyl]carbodiimide hydrochloride (EDAC, 2.74 g, 14.3 mmol). After stirring for 4 h at room temperature, the reaction mixture was washed with water and brine, dried over sodium sulfate, and filtered. Solvent was removed under reduced pressure to yield 1.15 g of the succinimidyl 4-azidobutyrate **3**.

Peptide Synthesis. Peptides were synthesized in the MIT Biopolymers Laboratory and their composition was confirmed via HPLC and mass spectrometry. The LyP-1 and LyP-1CTL peptides were synthesized with either heptynoic acid or propargylglycine at the N-terminus for conjugation. Each peptide is also labeled with a TAMRA fluorophore (Anaspec) via a lysine residue separated by an aminohexanoic acid (Ahx) spacer. (final sequence for LyP-1: Heptynoic acid or propargylglycine-K(Tamra)[Ahx]-CGNKRTRGC; for LyP-1CTL: Heptynoic acid or propargylglycine-K(Tamra)[Ahx]-CRVRTRSGC). Peptides were cyclized by bubbling air into 10 μM aqueous peptide solutions overnight. Finally, peptide solutions were lyophilized for subsequent use.

"Click" Attachment of Peptides to Nanoparticles. Succinimidyl 4-azidobutyrate was linked to 5 kDa thiol-PEG-amine polymers in 0.1 M HEPES 0.15 M NaCl pH 7.2 for 1 h at a 2:1 molar ratio between linker and polymer. Simultaneously, amino-modified, fluorochrome-labeled nanoparticles were activated with *N*-[γ-maleimidobutyryloxy] succinimide ester (GMBS) (dissolved in DMSO) cross-linker under similar conditions at a 200:1 molar ratio between cross-linker and nanoparticles. To remove excess GMBS, nanoparticle samples were filtered on a G50 column into 50 mM Na phosphate buffer at pH 7.2 supplemented with 10 mM EDTA. Purified nanoparticles were then combined with the polymer reaction mixture and allowed to react at room temperature overnight. Azido-PEG-nanoparticles were then purified from excess polymer and succinimidyl 4-azidobutyrate on a size exclusion column (ACA-44 media: Pall) into 0.1 M HEPES pH 7.2 buffer. Finally, the

Scheme 2. Synthesis of LyP-1-Coated Nanoparticles Using "Click" Chemistry[a]

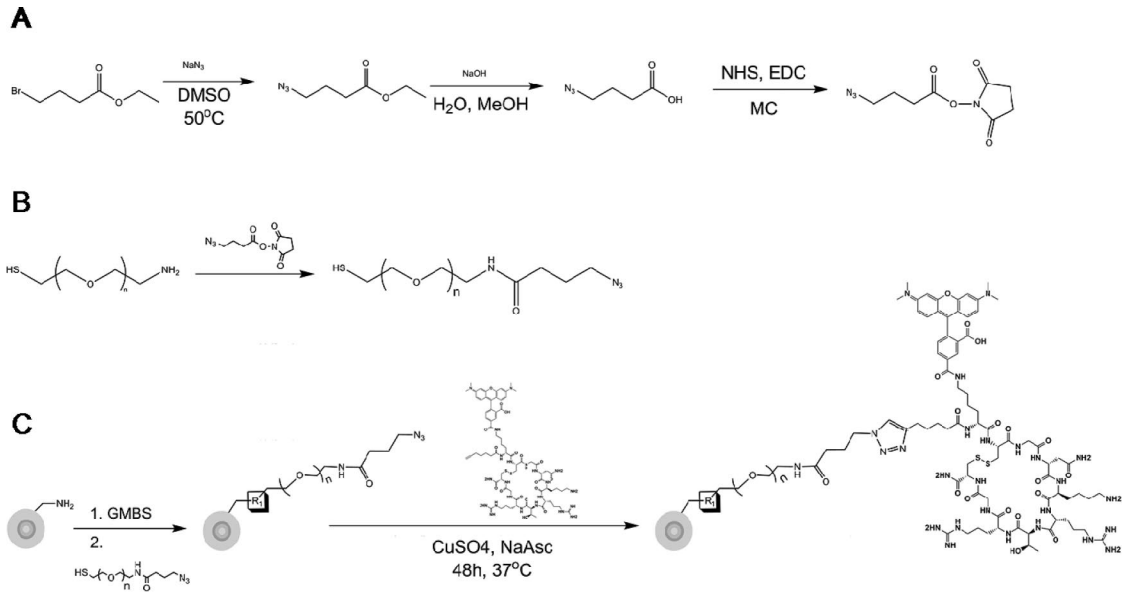

[a] (A) Synthesis of succinimidyl 4-azidobutyrate. (B) Synthesis of azide-PEG-thiol by linking succinimidyl 4-azidobutyrate to a 5 kDa thiol-PEG-amine. (C) Aminated, cross-linked, fluorochrome-labeled superparamagnetic iron-oxide nanoparticles are activated with GMBS, filtered, and then reacted with the thiol-PEG-azide from (B) to yield azido-PEG bearing nanoparticles. After purification, the particle solutions were reacted with alkyne-bearing LyP-1 peptides with $CuSO_4$/Na Ascorbate as catalysts to yield LyP-1-coated nanoparticles for *in vitro* and *in vivo* use.

azide-PEG-bearing particles were concentrated using Amicon Ultra-4 (Millipore) filters and stored at 4 °C.

To optimize catalyst concentrations for the "click" reaction by HPLC, a 10-fold excess of azido-PEG-NH_2 or *O*-(2-aminoethyl)-*O′*-(2-azidoethyl)pentaethylene glycol (Polypure) was added to a 100 μM peptide solution. $CuSO_4$ and Na ascorbate were dissolved in H_2O and added to the reaction mixture to final concentrations of 1 mM/5 mM and 10 mM/50 mM $CuSO_4$/Na Ascorbate. This mixture was shaken at 37 °C for various times (1 day to 3 days), after which it was characterized via HPLC.

Alkyne-bearing peptides (70:1 peptide/nanoparticle molar ratio), $CuSO_4$ (1 mM), and sodium ascorbate (5 mM) in H_2O were added to a solution of particles and the mixture was shaken at 37 °C for 48 h. Following the reaction, nanoparticles were purified from copper catalyst and excess peptides by filtration in ACA-44 size exclusion media into 0.1 M HEPES 0.15 M NaCl pH 7.2 buffer.

Cell Culture. Cell uptake experiments were performed using a human MDA-MB-435 cancer cell line. Grow media was minimum essential medium eagle (Invitrogen) with fetal bovine serum (10%; Invitrogen). Cells were passaged into 96-well plates and used at 60−80% confluency.

For peptide uptake experiments (Figure 1), LyP-1 or LyP-1CTL peptides were added to cell monolayers in serum-containing media at a final concentration of 10 μM. After 45 min of incubation at 37 °C, cells were washed with media, PBS, treated with trypsin (0.25%) and EDTA, and resuspended in 1% BSA (in PBS) for flow cytometry (BD LSRII). Fluorescence data on 10 000 cells was collected for each sample.

For nanoparticle uptake experiments (Figure 2), particles bearing an LyP-1, LyP-1CTL, or terminal azides were added to the cells in serum media at a final concentration of 100 nM. After 2 h of incubation, cells were trypsinized and assayed for particle fluorescence by flow cytometry. For peptide inhibition experiments, free LyP-1 peptides (10 μM to 100 μM) were first incubated with the cells for 1 h. The cells were then washed with media and 100 nM of LyP-1-coated nanoparticles were added to the cell culture. For imaging, cells were washed with PBS and observed using a 20× objective. Images were captured with a CCD camera mounted on a Nikon TE200 inverted epifluorescence microscope.

In Vivo Studies of Nanoparticle Targeting. Nude athymic mice were inoculated subcutaneously with human cancer cells (MDA-MB-435). After tumors had reached ~0.5 cm^3 in size, LyP-1- and azide-bearing nanoparticles were injected intravenously in the tail vein (1 mgFe/kg). Twenty-four hours after the injection, tumor tissues were excised, snap−frozen, and cut into 15 μm histological sections. Rat antimouse CD-31 (1:50, BD Pharmingen) and polyclonal anti-p32 antibody (1:200 (*34*)) were used for immunohistochemical staining of frozen tissue sections. The corresponding secondary antibodies were added and incubated for 1 h at room temperature: Alexa Fluor 594 goat antirat IgG (1:500, Invitrogen) for CD-31 and Alexa Fluor 594 goat antirabbit IgG (1:500, Invitrogen) for p32 antibody. The slides were washed three times with PBS and mounted in Vectashield Mounting Medium with DAPI (Vector Laboratories). The stained tumor sections were observed with a fluorescence microscope (Nikon, Tokyo, Japan). Histological quantitation of nanoparticles localization was done using *ImageJ* software. Stacks of CD31-stained sections and nanoparticle fluorescence images were utilized for intra- and extravascular particle distribution quantitation. Regions with CD31-staining were selected to denote intravascular accumulation of nanoparticles and surrounding areas were classified as extravascular. The net nanoparticle fluorescence signal above background was quantified for each of these regions to determine the approximate percent of nanoparticle fluorescence localized to the vasculature vs the extravascular space. Three sections from each set of mice were randomly chose for analysis.

RESULTS AND DISCUSSION

In order for "click" chemistry to be applied to the development of peptide-targeted nanomaterials, peptides must be able to harbor pendant alkyne or azide moieties without abating peptide activity. To investigate the efficacy of targeting peptides harboring pendant alkyne moieties, LyP-1 peptide (CGNKRTRGC) and untargeted cyclic control peptide, LyP-1CTL (CRVRTRSGC) in which the essential NKRTR motif is replaced with

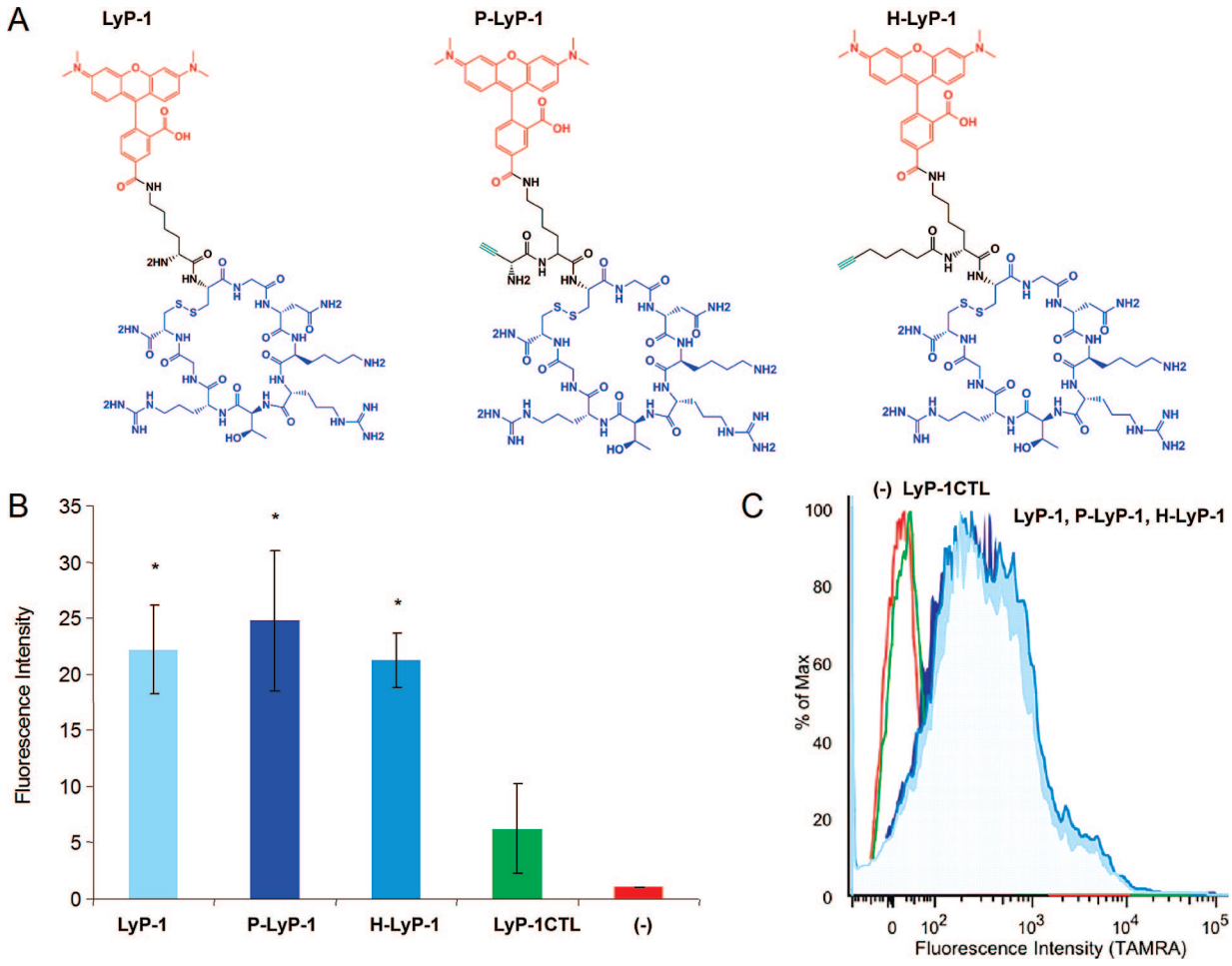

Figure 1. Native and alkyne-bearing LyP-1 peptides target p32-expressing MDA-MB-435 cells *in vitro*. (A) Structures of LyP-1, propargylglycine-LyP-1, and heptynoic acid-LyP-1, all labeled with a TAMRA fluorophore (red). The cyclic nonapeptide is in blue. The pendant alkyne moieties were conjugated to the N-terminus of the peptide during standard FMOC peptide synthesis. (B) Flow cytometry shows that peptides bearing different alkyne groups target MDA-MB-435 cancer cells similarly, while a scrambled control (LyP-1CTL) do not target (P = propargylglycine, H = 6-heptynoic acid, $*p < 0.01$, unpaired Student's *t*-test). (C) Flow cytometry histogram shows LyP-1, P-LyP-1, and H-LyP-1 peptides (in different shades of blue) target MDA-MB-435 cells *in vitro*, while LyP-1CTL peptide (green) did not show targeting relative to peptide-free control cells (red).

RVRTR to maintain net charge but abate p32 targeting (*33*), were synthesized to incorporate either of two alkyne moieties (the unnatural amino acid propargylglycine or 6-heptynoic acid) and a 5,6-carboxytetramethylrhodamine fluorophore (TAMRA) (Figure 1A; spectra: Supporting Information Figure 1). Because the alkyne moieties provide molecularly small chemical handles that may be incorporated in FMOC synthesis to either the N- or C-terminal of essential peptide sequences, we hypothesized their presence could be tailored to allow chemical attachment to azido-nanomaterials without interfering with LyP-1 peptide activity. In previous investigations, we found that N-terminal addition of visible and near-infrared fluorophores do not disrupt peptide binding to its receptors (*1, 33*). Accordingly, we reasoned alkyne moieties located near the N-terminus would be well-tolerated by the peptide (Figure 1A). To verify the specificity and efficacy of alkyne-LyP-1 targeting, 10 μM of LyP-1, bearing propargyl glycine, heptynoic, or no alkyne group were incubated for 45 min on monolayers of MDA-MB-435 human tumor cells, which have been shown to bind and internalize LyP-1 and express p32 at the cell surface (*33, 34*), LyP-1CTL peptides were included as a control sequence to verify targeted enhancement of uptake over nonspecific cyclic peptide structures. Cellular uptake of LyP-1 peptide was quantified via flow cytometry (Figure 1B) and plotted as the populational fluorescent intensity, relative to cells incubated with vehicle alone. *In vitro* targeting of LyP-1 peptides bearing either propargylglycine or 6-heptyoic acid was similar to that of native LyP-1 and control peptides (Figure 1C), indicating that alkyne modifications N-terminal to targeting sequences were innocuously chaperoned by peptides and did not affect cell binding.

We next probed the effect of three variables on "click" reaction conditions between our peptides and an azido-PEG-amine (catalyst, catalyst concentration, and reaction time). Azido-PEG-amine was chosen to emulate the azido-PEG surface of the nanoparticles to be used subsequently and to provide a model reaction amenable to HPLC quantitation of product formation. Copper(I) catalyst was added either directly as an iodinated salt (Cu(I)I), or indirectly as soluble copper sulfate ($Cu(II)SO_4$) and reduced by sodium ascorbate *in situ*. The degree of product formation was measured via HPLC with mass spectrometric verification of product identity. The addition of the azido-PEO-amine rendered peptides more hydrophilic and decreased retention times compared to unconjugated peptides. As shown in Supporting Information Table S1, product formation proceeded more completely in the tested reaction conditions for the heptynoic acid-LyP-1, likely due to reduced steric hindrance provided by the extended hydrocarbon chain. Optimal reaction conditions were found to be either 1 mM $CuSO_4$/5 mM Na ascorbate or 1 mM −100 mM CuI for 72 h. Notably, the reaction yields with 10 mM $CuSO_4$ levels were dramatically

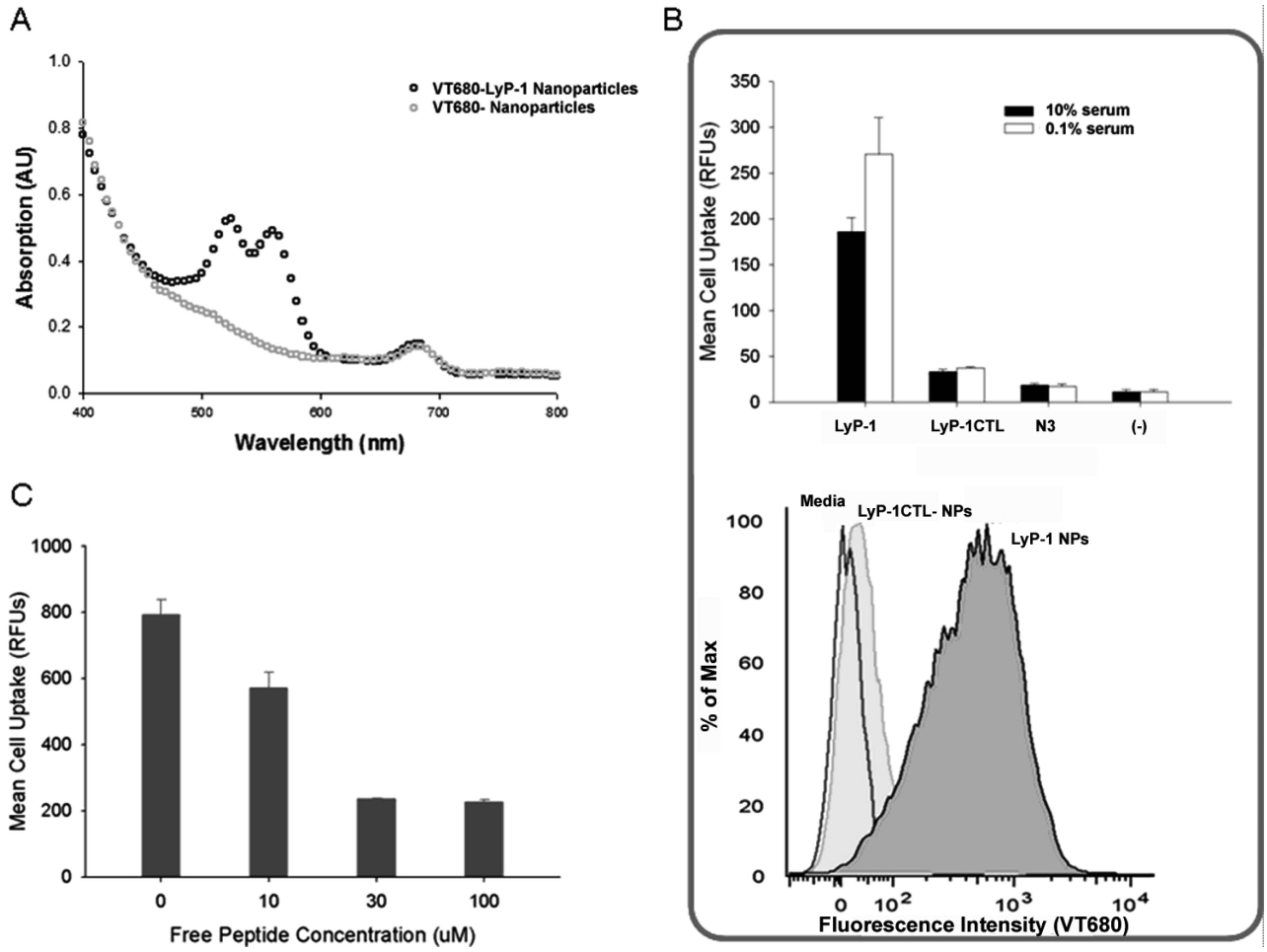

Figure 2. LyP-1-conjugated nanoparticles target p32-expressing MDA-MB-435 cells *in vitro*, while nanoparticles conjugated to control cyclic peptides (LyP-1CTL) do not target. (A) The amount of peptide bound per particle was quantified spectrophotometrically by measuring the absorbance of the TAMRA dyes added following the click reaction. With the addition of catalyst $CuSO_4$/Na ascorbate (dark circles), the TAMRA absorbance at 555 nm was quantified to equal approximately 30 peptides per particle, whereas no TAMRA signal was observed without catalyst (light circles). (B) LyP-1-nanoparticles or control LyP-1CTL-nanoparticles (both at ~30 peptides per particle), or parent azido-bearing particles (N3), were added to MDA-435-MB cancer cells in normal 10% serum (black bars) and 0.1% serum-starved (light bars) conditions. Flow cytometry histogram shows marked increase in uptake of LyP-1-nanoparticles (black contour) vs LyP-1CTL-nanoparticles (light gray contour) and particle-free control cells (dark gray contour). Each error bar represents 6 parallel experiments. (C) Addition of free LyP-1 peptides at concentrations from 10 to 100 uM inhibited cellular uptake of LyP-1-coated nanoparticles, suggesting that the LyP-1 peptide and LyP-1-labeled particles target the same receptor.

lower than 1 mM, likely due to global precipitation of reduced Cu(I) in solution. Nevertheless, we found 1 mM $CuSO_4$ reactions to yield more reliable conjugations than 1 to100 mM CuI reactions, possibly because the insolubility of CuI in aqueous solutions produced variations in the amount of available catalyst delivered to the reactions. Therefore, the optimal conditions for subsequent nanoparticle modification were determined to be 1 mM $CuSO_4$ and 5 mM Na ascorbate. Under these conditions, we did not observe any reduction of peptide disulfide bonds due to copper catalyst or Na ascorbate reduction as determined by MALDI mass spectrometry and HPLC analysis (data not shown).

Having verified that alkyne-bearing LyP-1 peptides could effectively target p32-expressing MDA-MB-435 cancer cells and become linked to azido-bearing PEG polymers, we next developed a protocol for linking these peptides onto azido-PEG bearing, near-infrared fluorochrome-labeled (VivoTag 680) iron oxide nanoparticles. Dextran-caged iron oxide nanoparticles were used as the parent formulation to provide a highly stable, relatively noncytotoxic, and *in vivo*-tested nanoparticle scaffold. Briefly, a heterobifunctional linker bearing an azide on one end an N-hydroxysuccinimide leaving group on the other was synthesized and attached to an amine-PEG-thiol polymer (MW 5000 Da) via its terminal amine (Scheme 2A,B). Azido-PEG-thiol polymers were subsequently linked to surface of cross-linked, aminated, and fluorochrome-labeled dextran-coated iron oxide nanoparticles via the linker *N*-[γ-maleimidobutyryloxy] succinimide ester (GMBS) (Scheme 2C). Long PEG polymers were utilized to carry pendant azide groups in order to enhance particle circulation time *in vivo* and to provide a generalizable nanoparticle surface, whereby optimized "click" attachment conditions might be applicable to other PEG-coated organic and inorganic nanomaterials in the future. Azido-PEG particles were purified from excess polymer and linked to alkyne-bearing peptides in 1 mM $CuSO_4$, 5 mM Na ascorbate. Finally, the conjugated nanoparticles were purified and sterile filtered for *in vitro* and *in vivo* applications.

Peptide valency on nanoparticles was assessed spectrophotometrically by quantifying the number of TAMRA dyes added onto nanoparticles following "click" reaction (Figure 2A). In the presence of catalyst, approximately 30 peptides were added per nanoparticle for both LyP-1 and LyP-1CTL peptides, whereas no addition was observed in the absence of catalyst (Figure 2A). LyP-1 nanoparticles, LyP-1CTL nanoparticles, or azide nanoparticles were incubated over MDA-MB-435 tumor cells for 2 h and nanoparticle accumulation was quantified using flow cytometry (Figure 2B). LyP-1-nanoparticles showed significant tumor cell accumula-

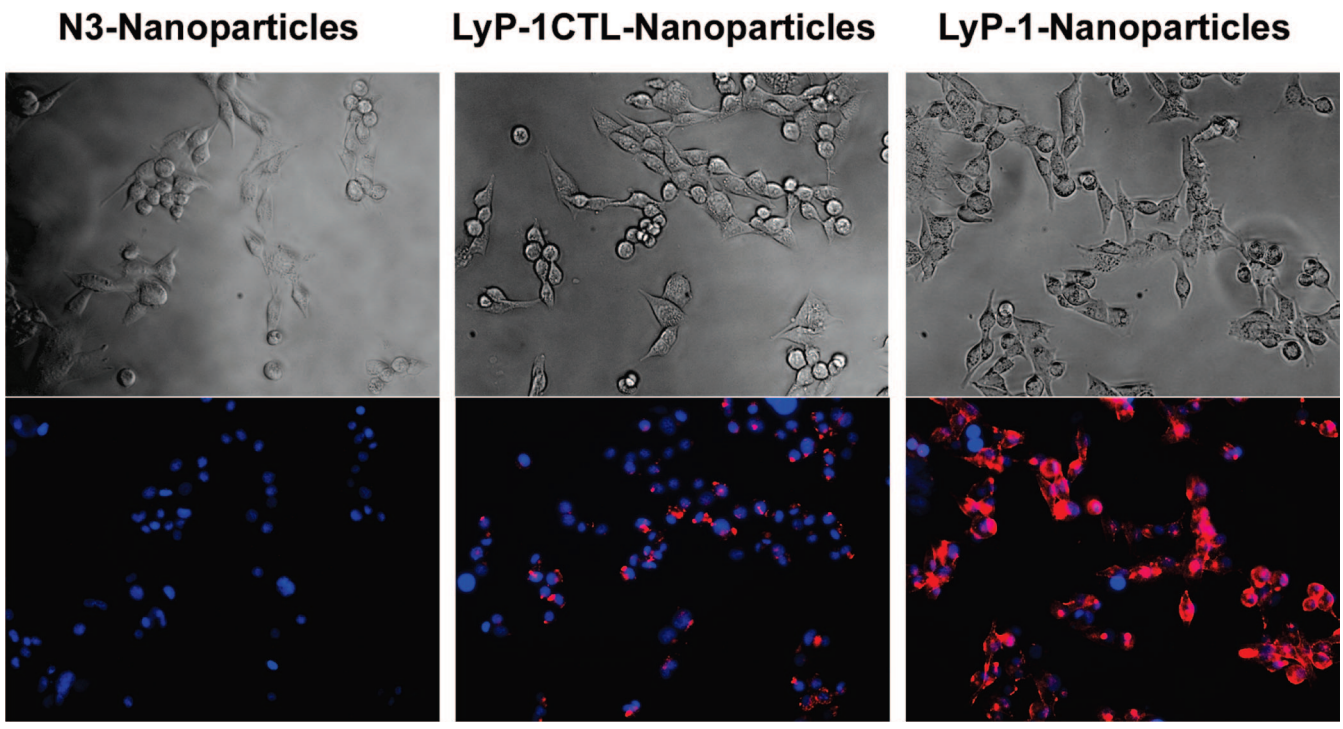

Figure 3. LyP-1-nanoparticles target MDA-MB-435 cancer cells (right). Fluorescence imaging of cells incubated with LyP-1-nanoparticles showed increased near-infrared fluorescence (red). Uptake of azido-bearing or scrambled control peptide (LyP-1CTL)-bearing nanoparticles are not visible or show minor background (left and middle).

tion, while LyP-1CTL-nanoparticles or azide-nanoparticles displayed minimal cell uptake (Figure 2B). The effect of serum on nanoparticle uptake was also studied, as low serum levels enhance the stress-induced expression of the p32 receptor (*33*). The slight increase in LyP-1-nanoparticle targeting in lower serum levels provided further validation of receptor-specific targeting, as decreased serum protein concentrations lowers the likelihood of nonspecific serum protein mediated uptake. To further confirm the uptake specificity of LyP-1-nanoparticles, free LyP-1 peptide was added to cells along with LyP-1-particles (Figure 2C). Dose-dependent inhibition of uptake was observed with LyP-1 peptide concentrations from 10 to 100 μM, suggesting the free LyP-1 and LyP-1-labeled particles share common cellular receptors. We attribute the large excess of free peptide required for inhibition compared to the concentration of nanoparticles used (100 nM) to the presence of multiple copies of the LyP-1 peptide on each nanoparticle, thus improving nanoparticle avidity to receptors through polyvalent binding (*38*). In order to visualize LyP-1 peptide-mediated cell uptake, nanoparticles bearing pendant LyP-1 peptides, control LyP-1CTL peptides, or azides were incubated over MDA-MB-435 cells for 30 min, washed, incubated with a nuclear stain, and imaged via epifluorescence microscopy (Figure 3). LyP-1-nanoparticles were seen associated with cells, while markedly less binding of azide-bearing or control peptide-bearing nanoparticles was not observed. If the same staining procedure was instead performed at 24 h post-incubation, LyP-1-nanoparticles were seen in punctate locations consistent with sequestration in endosome-like compartments (Supporting Information Figure 2). To assess the cytotoxicity of "click" nanoparticles, NH_2-PEG-, azido-PEG-, and peptide-conjugated nanoparticles were incubated for 24 h above HeLa cell cultures (Supporting Information Figure 3). In all three formulations, the TC50 is >7 mM Fe, or over 16 times higher than maximal blood concentrations during *in vivo* experiments performed here and 32 times higher than concentrations used *in vitro* here.

Having found that "click" attachment of homing peptides could mediate the targeting nanoparticles *in vitro*, we evaluated the ability of "click" chemistry to direct nanoparticle targeting to specific tumor cells *in vivo*. Again, near-infrared fluorochrome-labeled (VivoTag 680) nanoparticles were "clicked" to LyP-1 peptides, resulting on average of ~30 LyP-1 peptides per particle, while the parent azido-PEG nanoparticles were used as a negative control. Each population of nanoparticles was injected intravenously into mice bearing human MDA-MB-435 cancer xenografts. Nanoparticles were allowed to circulate and distribute in mice for 24 h, after which the mice were sacrificed and organs collected for immunohistochemical or whole organ fluorescence analysis. Vascular staining with anti-CD31 antibodies showed that azide nanoparticles in tumors remained localized within the immediate periphery of blood vessels (Figure 4B). This perivascular distribution of untargeted nanomaterials is in agreement with previous histological and intravital observations of passive liposomal accumulation in tumors (*39, 40*). By contrast, LyP-1 "click" nanoparticles appeared to have extravasated from the tumor vasculature, penetrated into the interstitial space of the tumor, and bound to p32-expressing cells (Figure 4B,C). As a result, the fraction of LyP-1 nanoparticles that get sequestered beyond the perivascular space was significantly higher than that of azido nanoparticles (Figure 4D) ($P < 0.005$). This pattern was observed in all injected mice and is characteristic of LyP-1 peptide and phage homing observed previously (*1*). Interestingly, previous LyP-1 bacteriophage experiments showed that the LyP-1-expressing phage concentrate in nonvascularized sites of tumors within minutes after injection while insertless phage do not reach these regions (*1*). Thus, there may be unique transportation pathways within tumors that are exploited by this ligand after extravasation that are not available to untargeted materials. In the future, the localization of LyP-1 nanoparticles in avascular tumor regions may be of use for directing therapeutics into hypoxic regions of tumors, where most nanoparticle therapies do not reach. Whole organ assessment

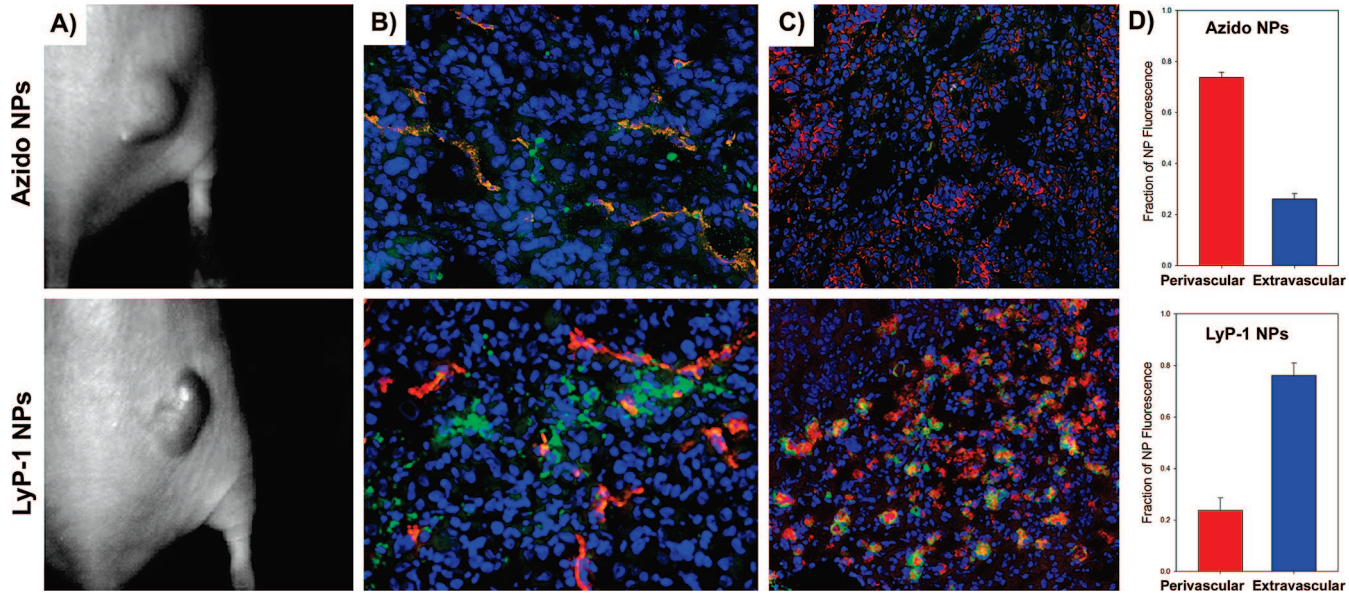

Figure 4. "Click" LyP-1-nanoparticle targeting to tumor cells *in vivo*. Nanoparticles bearing only azide groups (top) or labeled with LyP-1 peptides (bottom) that are matched in circulation time were injected intravenously via the tail vein into mice bearing human MDA-MB-435 cancer xenografts. Histological sections were obtained 24 h postinjection. (A) Light reflectance images of mice bearing the tumor xenografts. (B) Fluorescent LyP-1-nanoparticles (VT680 fluorescence pseudocolored as green) did not colocalize with CD31, a blood vessel marker (red), while untargeted azide-PEG nanoparticles remained localized to the blood vessels or their immediate periphery. (C) LyP-1-nanoparticles (green) accumulated in regions of high p32 expression (red), whereas untargeted, azido-bearing nanoparticles did not accumulate in these areas. (D) Histological quantitation using CD31 stain to assess nanoparticle localization to immediate periphery of blood vessels. The fraction of LyP-1 nanoparticles outside of the perivascular space of CD31-stained blood vessels is significantly higher than azido-nanoparticles ($P < 0.005$) as assessed from three randomly chosen views in each set of mice ($n = 3$). Together, LyP-1-coated nanoparticles penetrate into the tumor interstitium to target p32-expressing cells.

of near-infrared tumor fluorescence demonstrated that, despite the distinct microscopic behavior of LyP-1 nanoparticles, the macroscopic tumor accumulation of LyP-1 nanoparticles and PEG-azide nanoparticles was similar (Supporting Information Figure 4), indicating that the targeted accumulation of LyP-1-nanoparticles was on par with passive delivery, whereby long-circulating materials accumulate in tumors via their hyperporous vasculature over time (*41, 42*). These results are in accordance with data showing that the development of targeted nanoparticle formulations that amplify the macroscopic accumulation in tumors requires systematic *in vivo* optimization of multiple material parameters, including target avidity, circulation time, and particle size (*43, 44*). Experiments of this kind are ongoing in order to probe the power of the LyP-1 targeting ligand for amplifying the accumulation and efficacy of nanoparticle-based imaging and therapeutic agents.

CONCLUSION

In this work, we have demonstrated that "click" chemistry may be used to develop nanoparticles that seek out specific cells *in vivo* based on their surface expression of protein markers. Ultimately, these findings suggest that "click" chemistry meets the criteria of being applicable under aqueous conditions, efficient, orthogonal to thiol- and amine-containing targeting motifs, and stable in the complex *in vivo* environments of the blood and tumor milieu. In the future, this work may empower the development of "click" nanomaterials that seek out specific tumor cell types, including tumor stem cells and angiogenic endothelial cells, or amplify the macroscopic accumulation of imaging agents or therapeutics in tumors. Further, the modularity of this "click" attachment strategy should allow it to be adapted to a diversity of *in vivo* nanoparticle platforms and both biological and synthetic ligands, potentially empowering novel on-nanoparticle screen approaches to targeted nanomaterial development.

ACKNOWLEDGMENT

The authors acknowledge financial support from NIH (BRP: 1R01CA124427-01), NIH/NCI (U54 CA119349-01, U54 CA119335), Packard Fellowship (1999-1453A), Whitaker Foundation Graduate Fellowship (G. v. M.), NSF Graduate Fellowship (G. v. M.), and Medical Scientist Training Program (Y.R.). The authors declare no competing financial interests.

Supporting Information Available: Studies on the optimization of the "click" reaction by HPLC, LyP-1 peptide spectra, localization of LyP-1 nanoparticles in endosomal-like compartments, nanoparticle cytotoxicity, and LyP-1 and azido nanoparticle tumor accumulation. This material is available free of charge via the Internet at http://pubs.acs.org.

LITERATURE CITED

(1) Laakkonen, P., Porkka, K., Hoffman, J. A., and Ruoslahti, E. (2002) A tumor-homing peptide with a targeting specificity related to lymphatic vessels. *Nat. Med. 8*, 751–5.
(2) Lee, S. M., Lee, E. J., Hong, H. Y., Kwon, M. K., Kwon, T. H., Choi, J. Y., Park, R. W., Kwon, T. G., Yoo, E. S., Yoon, G. S., Kim, I. S., Ruoslahti, E., and Lee, B. H. (2007) Targeting bladder tumor cells in vivo and in the urine with a peptide identified by phage display. *Mol. Cancer Res. 5*, 11–9.
(3) Rajotte, D., and Ruoslahti, E. (1999) Membrane dipeptidase is the receptor for a lung-targeting peptide identified by in vivo phage display. *J. Biol. Chem. 274*, 11593–8.
(4) Porkka, K., Laakkonen, P., Hoffman, J. A., Bernasconi, M., and Ruoslahti, E. (2002) A fragment of the HMGN2 protein homes to the nuclei of tumor cells and tumor endothelial cells in vivo. *Proc. Natl. Acad. Sci. U.S.A. 99*, 7444–9.
(5) Ruoslahti, E. (2004) Vascular zip codes in angiogenesis and metastasis. *Biochem. Soc. Trans. 32*, 397–402.
(6) Simberg, D., Duza, T., Park, J. H., Essler, M., Pilch, J., Zhang, L., Derfus, A. M., Yang, M., Hoffman, R. M., Bhatia, S., Sailor, M. J., and Ruoslahti, E. (2007) Biomimetic amplification of

nanoparticle homing to tumors. *Proc. Natl. Acad. Sci. U.S.A. 104*, 932–6.

(7) Reddy, G. R., Bhojani, M. S., McConville, P., Moody, J., Moffat, B. A., Hall, D. E., Kim, G., Koo, Y. E., Woolliscroft, M. J., Sugai, J. V., Johnson, T. D., Philbert, M. A., Kopelman, R., Rehemtulla, A., and Ross, B. D. (2006) Vascular targeted nanoparticles for imaging and treatment of brain tumors. *Clin. Cancer Res. 12*, 6677–86.

(8) Zhang, C., Jugold, M., Woenne, E. C., Lammers, T., Morgenstern, B., Mueller, M. M., Zentgraf, H., Bock, M., Eisenhut, M., Semmler, W., and Kiessling, F. (2007) Specific targeting of tumor angiogenesis by RGD-conjugated ultrasmall superparamagnetic iron oxide particles using a clinical 1.5-T magnetic resonance scanner. *Cancer Res. 67*, 1555–62.

(9) Weissleder, R., Kelly, K., Sun, E. Y., Shtatland, T., and Josephson, L. (2005) Cell-specific targeting of nanoparticles by multivalent attachment of small molecules. *Nat. Biotechnol. 23*, 1418–23.

(10) Giordano, R. J., Anobom, C. D., Cardo-Vila, M., Kalil, J., Valente, A. P., Pasqualini, R., Almeida, F. C., and Arap, W. (2005) Structural basis for the interaction of a vascular endothelial growth factor mimic peptide motif and its corresponding receptors. *Chem. Biol. 12*, 1075–83.

(11) Colombo, G., Curnis, F., DeMori, G. M., Gasparri, A., Longoni, C., Sacchi, A., Longhi, R., and Corti, A. (2002) Structure-activity relationships of linear and cyclic peptides containing the NGR tumor-homing motif. *J. Biol. Chem. 277*, 47891–7.

(12) Rozek, A., Powers, J. P., Friedrich, C. L., and Hancock, R. E. (2003) Structure-based design of an indolicidin peptide analogue with increased protease stability. *Biochemistry 42*, 14130–8.

(13) Ruoslahti, E., and Pierschbacher, M. D. (1987) New perspectives in cell adhesion: RGD and integrins. *Science 238*, 491–7.

(14) Green, J. J., Chiu, E., Leshchiner, E. S., Shi, J., Langer, R., and Anderson, D. G. (2007) Electrostatic ligand coatings of nanoparticles enable ligand-specific gene delivery to human primary cells. *Nano Lett. 7*, 874–9.

(15) Sokolov, K., Follen, M., Aaron, J., Pavlova, I., Malpica, A., Lotan, R., and Richards-Kortum, R. (2003) Real-time vital optical imaging of precancer using anti-epidermal growth factor receptor antibodies conjugated to gold nanoparticles. *Cancer Res. 63*, 1999–2004.

(16) Huang, X., El Sayed, I. H., Qian, W., and El Sayed, M. A. (2006) Cancer cell imaging and photothermal therapy in the near-infrared region by using gold nanorods. *J. Am. Chem. Soc. 128*, 2115–20.

(17) Kolb, H. C., Finn, M. G., and Sharpless, K. B. (2001) Click Chemistry: Diverse Chemical Function from a Few Good Reactions. *Angew. Chem., Int. Ed. 40*, 2004–2021.

(18) Lee, J. W., Kim, J. H., Kim, H. J., Han, S. C., Kim, J. H., Shin, W. S., and Jin, S. H. (2007) Synthesis of symmetrical and unsymmetrical PAMAM dendrimers by fusion between azide- and alkyne-functionalized PAMAM dendrons. *Bioconjugate Chem. 18*, 579–84.

(19) Wu, P., Malkoch, M., Hunt, J. N., Vestberg, R., Kaltgrad, E., Finn, M. G., Fokin, V. V., Sharpless, K. B., and Hawker, C. J. (2005) Multivalent, bifunctional dendrimers prepared by click chemistry. *Chem. Commun. (Cambridge)* 5775–7.

(20) Shi, Q., Chen, X., Lu, T., and Jing, X. (2008) The immobilization of proteins on biodegradable polymer fibers via click chemistry. *Biomaterials 29*, 1118–26.

(21) Rozkiewicz, D. I., Gierlich, J., Burley, G. A., Gutsmiedl, K., Carell, T., Ravoo, B. J., and Reinhoudt, D. N. (2007) Transfer printing of DNA by "click" chemistry. *ChemBioChem 8*, 1997–2002.

(22) Ciampi, S., Bocking, T., Kilian, K. A., James, M., Harper, J. B., and Gooding, J. J. (2007) Functionalization of acetylene-terminated monolayers on Si(100) surfaces: a click chemistry approach. *Langmuir 23*, 9320–9.

(23) Such, G. K., Tjipto, E., Postma, A., Johnston, A. P., and Caruso, F. (2007) Ultrathin, responsive polymer click capsules. *Nano Lett 7*, 1706–10.

(24) Li, H., Cheng, F., Duft, A. M., and Adronov, A. (2005) Functionalization of single-walled carbon nanotubes with well-defined polystyrene by "click" coupling. *J. Am. Chem. Soc. 127*, 14518–24.

(25) Cavalli, S., Tipton, A. R., Overhand, M., and Kros, A. (2006) The chemical modification of liposome surfaces via a copper-mediated [3 + 2] azide-alkyne cycloaddition monitored by a colorimetric assay. *Chem. Commun. (Cambridge)* 3193–5.

(26) Fischler, M., Sologubenko, A., Mayer, J., Clever, G., Burley, G., Gierlich, J., Carell, T., and Simon, U. (2008) Chain-like assembly of gold nanoparticles on artificial DNA templates via 'click chemistry'. *Chem. Commun. (Cambridge)* 169–71.

(27) Opsteen, J. A., Brinkhuis, R. P., Teeuwen, R. L., Lowik, D. W., and van Hest, J. C. (2007) "Clickable" polymersomes. *Chem. Commun. (Cambridge)* 3136–8.

(28) Antoni, P., Nystrom, D., Hawker, C. J., Hult, A., and Malkoch, M. (2007) A chemoselective approach for the accelerated synthesis of well-defined dendritic architectures. *Chem. Commun. (Cambridge)* 2249–51.

(29) Zeng, Q., Li, T., Cash, B., Li, S., Xie, F., and Wang, Q. (2007) Chemoselective derivatization of a bionanoparticle by click reaction and ATRP reaction. *Chem. Commun. (Cambridge)* 1453–5.

(30) Brennan, J. L., Hatzakis, N. S., Tshikhudo, T. R., Dirvianskyte, N., Razumas, V., Patkar, S., Vind, J., Svendsen, A., Nolte, R. J., Rowan, A. E., and Brust, M. (2006) Bionanoconjugation via click chemistry: The creation of functional hybrids of lipases and gold nanoparticles. *Bioconjugate Chem. 17*, 1373–5.

(31) Sun, E. Y., Josephson, L., and Weissleder, R. (2006) "Clickable" nanoparticles for targeted imaging. *Mol. Imaging 5*, 122–8.

(32) Said Hassane, F., Frisch, B., and Schuber, F. (2006) Targeted liposomes: convenient coupling of ligands to preformed vesicles using "click" chemistry. *Bioconjugate Chem. 17*, 849–54.

(33) Laakkonen, P., Akerman, M. E., Biliran, H., Yang, M., Ferrer, F., Karpanen, T., Hoffman, R. M., and Ruoslahti, E. (2004) Antitumor activity of a homing peptide that targets tumor lymphatics and tumor cells. *Proc. Natl. Acad. Sci. U.S.A. 101*, 9381–6.

(34) Fogal, V., Zhang, L., and Ruoslahti, E. Mitochondrial/cell surface protein p32/gC1qR as a molecular target in tumor cells and tumor stroma. *Cancer Res*. (Submitted).

(35) Rubinstein, D. B., Stortchevoi, A., Boosalis, M., Ashfaq, R., Ghebrehiwet, B., Peerschke, E. I., Calvo, F., and Guillaume, T. (2004) Receptor for the globular heads of C1q (gC1q-R, p33, hyaluronan-binding protein) is preferentially expressed by adenocarcinoma cells. *Int. J. Cancer 110*, 741–50.

(36) Shen, T., Weissleder, R., Papisov, M., Bogdanov, A., Jr., and Brady, T. J. (1993) Monocrystalline iron oxide nanocompounds (MION): physicochemical properties. *Magn. Reson. Med. 29*, 599–604.

(37) Josephson, L., Tung, C. H., Moore, A., and Weissleder, R. (1999) High-efficiency intracellular magnetic labeling with novel superparamagnetic-Tat peptide conjugates. *Bioconjugate Chem. 10*, 186–91.

(38) Montet, X., Funovics, M., Montet-Abou, K., Weissleder, R., and Josephson, L. (2006) Multivalent effects of RGD peptides obtained by nanoparticle display. *J. Med. Chem. 49*, 6087–93.

(39) Unezaki, S., Maruyama, K., Hosoda, J., Nagae, I., Koyanagi, Y., Nakata, M., Ishida, O., Iwatsuru, M., and Tsuchiya, S. (1996) Direct measurement of the extravasation of polyethyleneglycol-coated liposomes into solid tumor tissue by in vivo fluorescence microscopy. *Int. J. Pharm. 144*, 11–17.

(40) Son, D. H., Park, S. A., Lee, S. W., Cho, Y. W., Roh, J. L., and Kim, S. Y. (2006) In vivo tumor targeting and radionuclide imaging with self-assembled nanoparticles: Mechanisms, key factors, and their implications. *EJC Suppl. 4*, 47–47.

(41) Moghimi, S. M., and Szebeni, J. (2003) Stealth liposomes and long circulating nanoparticles: critical issues in pharmacokinetics,

opsonization and protein-binding properties. *Prog. Lipid Res. 42*, 463–78.

(42) Moghimi, S. M., Hunter, A. C., and Murray, J. C. (2001) Long-circulating and target-specific nanoparticles: theory to practice. *Pharmacol. Rev. 53*, 283–318.

(43) Bartlett, D. W., Su, H., Hildebrandt, I. J., Weber, W. A., and Davis, M. E. (2007) Impact of tumor-specific targeting on the biodistribution and efficacy of siRNA nanoparticles measured by multimodality in vivo imaging. *Proc. Natl. Acad. Sci. U.S.A. 104*, 15549–54.

(44) Gu, F., Zhang, L., Teply, B. A., Mann, N., Wang, A., Radovic-Moreno, A. F., Langer, R., and Farokhzad, O. C. (2008) Precise engineering of targeted nanoparticles by using self-assembled biointegrated block copolymers. *Proc. Natl. Acad. Sci. U.S.A. 105*, 2586–2591.

BC800077Y